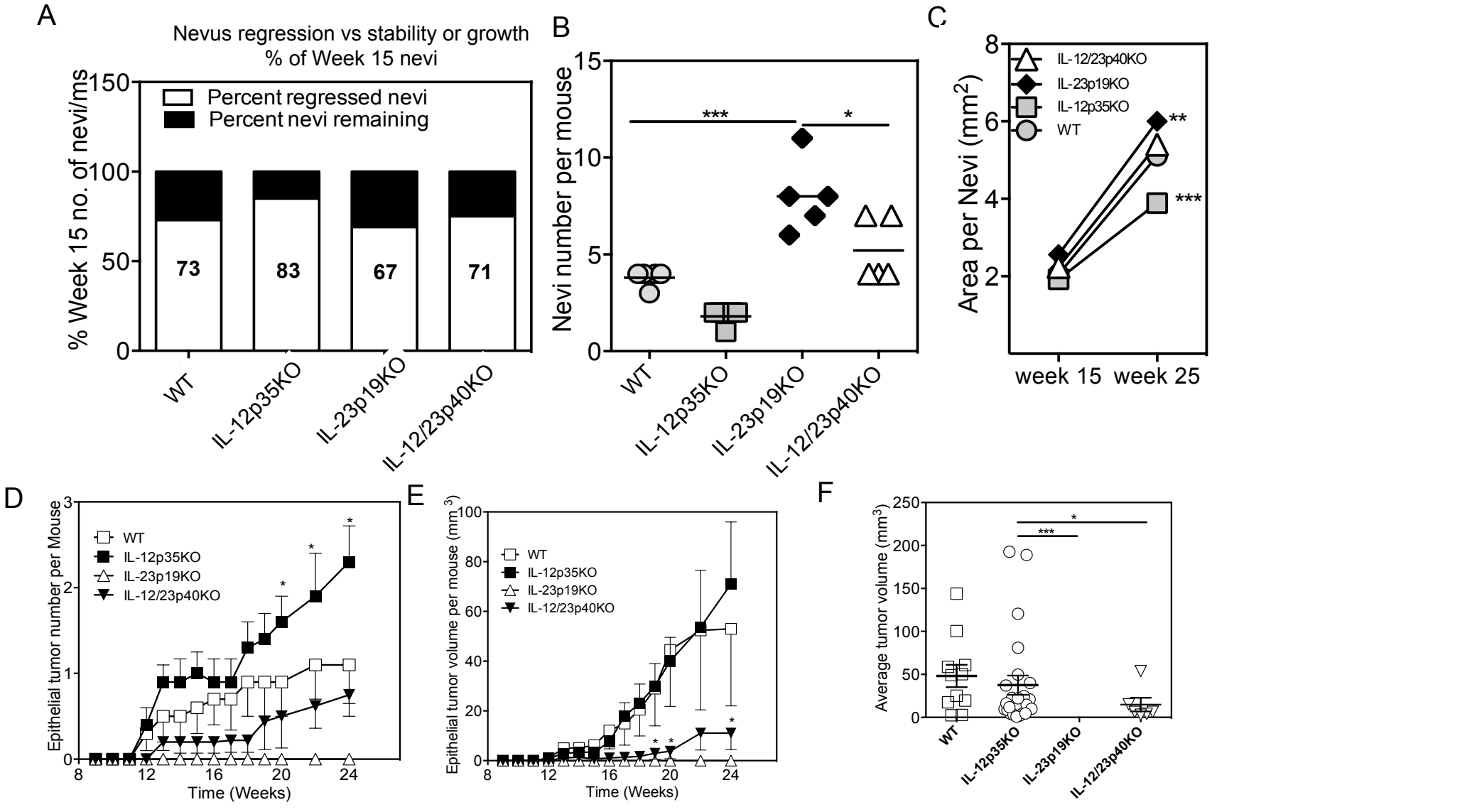

Supplementary Figure 1. IL-23 inhibits nevus growth in the absence of TPA and promotes SCC development (A) Percentage of nevi remaining at week 25 after cessation of TPA on week 15 (black area). Numbers represent percent regression. **(B)** Number of nevi per mouse at week 25, after 10 weeks without TPA. **(C)** Continued nevus growth without TPA**.** Individual nevi were monitored following TPA withdrawal over 10 weeks. All stable non-regressing lesions grew continuously. Lesions grew at an accelerated pace in the absence of IL-23, while in the absence of IL-12, lesion growth rate was significantly slower. *p is <0.05. ***is p<0.001. Age matched WT mice and KO mice underwent chemical carcinogenesis for 24 weeks. SCCs were counted and volume measured weekly. **(D)** Epithelial tumor development kinetics. IL-12p35KO mice developed nearly 2 times more epithelial tumors as compared to WT mice. IL-23p19KO mice were completely resistant to the SCC tumor development. **(E)** Epithelial tumor growth kinetics in WT and KO mice. **(F)** Average tumor volume attained in WT and KO mice at week 24. *p is <0.05. ***is p<0.001

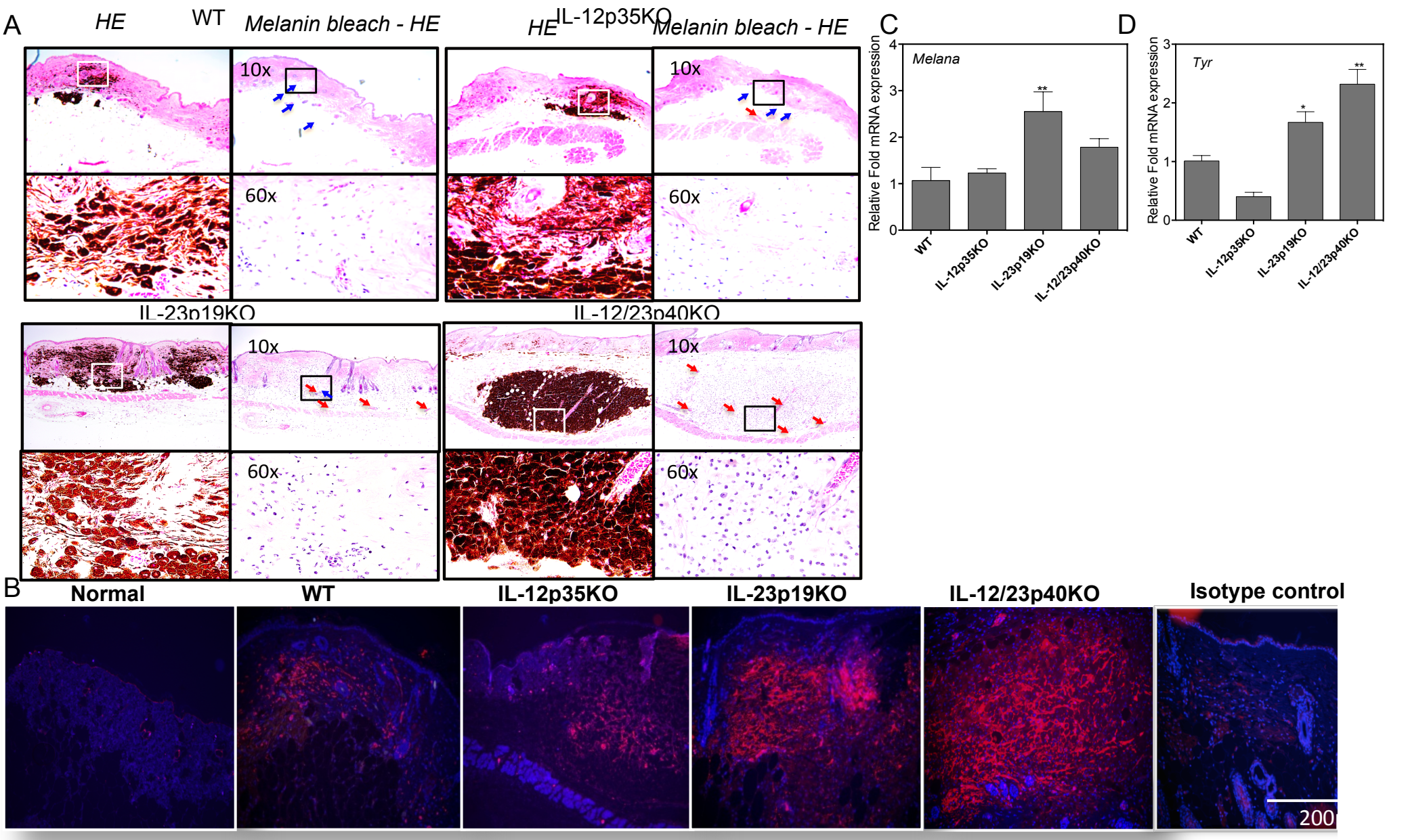

Supplementary Figure 2. Nevi from IL-23p19KO and IL-12/23p40KO mice show enhanced melanocytic lineage marker expression compared to WT and IL-12p35KO mice. (A) Panels of H & E stained nevi tissue serial section pairings of unbleached (left) and bleached (right) views taken with objective magnification of 10x or 60x as shown. Patterns differed in that enhanced angiogenesis (Red arrow) but fewer infiltrating inflammatory cells (blue arrow) in lesions from IL-23p19KO and IL-12/23p40KOs as compared to WT or IL-12p35KO mice. **(B)** The sections were stained with anti-mouse S100 antibody [clone 4C4.9] or isotype control. All the slides were incubated with DyLight 594 Donkey anti-mouse IgG. All sections were counterstained with DAPI to stain nuclei. The photomicrographs were taken with a 20x objective lens. **(C & D)** Real-time PCR analysis of lesional tissues from all groups of mice. The pigmented tissues were removed and processed as described in the Materials and Methods. cDNA was analyzed for Melan A and tyrosinase expression as described in Materials and Methods. ** is $p<0.01$.

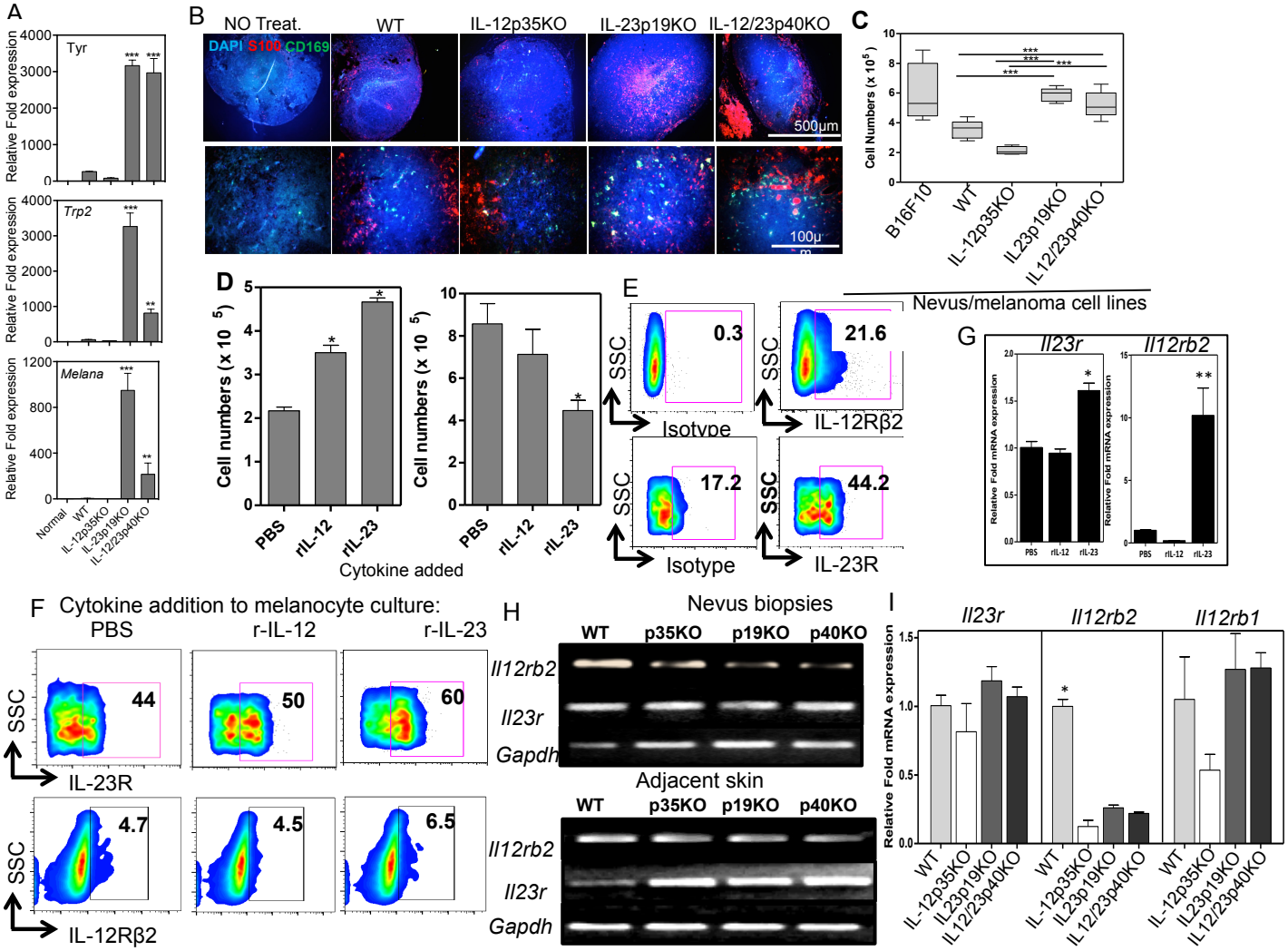

Supplementary Figure 3. (A) Increased melanocyte gene expression in LNs of DMBA/TPA treated mice (B) S100 positive LN cells are discrete from myeloid cells or macrophage subsets. The red areas indicate melanoma cells that have migrated to the LNs. There is increased macrophage density in LNs of IL-23p19KO and IL-12/23p40KO mice. **(C)** Cell lines were suspended in 6-well plates at $1x10^5$/ml and 48h later cells were counted in each group. **(D)** IL-23 and IL-12 at 300 ng/ml was added to $1x10^5$ cells per well in a 6-well plate. Cells were counted 48 hours later. The control cultures did not receive cytokines (n=4/group). Viability was comparable in all cultures, >95%. *p is <0.05. ***is p<0.001. **(E)** Normal melanocytes were cultured in melanocyte specific media and after 24h, cells were stained with PE-anti-IL-12Rβ2 (Clone 305719) or rabbit anti-IL-23R (CAT# IMG-5092A). To detect IL-23R, FITC anti-Rabbit antibody was used and expression detected by flow cytometry. **(F & G)** Melanocytes were cultured in melanocyte specific media in presence or absence of IL-23 or IL-12 (100 µg/ml) for: **(F)** 24h and analyzed for IL-23R and IL-12Rβ2 expression by flow cytometry or **(G)**12h and mRNA **(H)** Nevus biopsies or adjacent skin from all the indicated groups of mice was isolated, scraped of subcutaneous fat. Nevus biopsies were incubated in dispase for 30 minutes at 37°C. to remove epidermis and then RNA extracted as described in Materials and Methods. Then RT PCR for IL-23R or IL-12Rβ2 was done to detect the receptors. RT-PCR analysis of IL-23R or IL-12Rβ2 in skin that was treated with TPA, but was free of melanocytic nevi, was also done. **(I)** Real-time PCR analysis of IL-23R, IL-12Rβ2 and the common IL-12Rβ1 shared by both IL-12 receptor and IL-23 receptor. *p is <0.05. **is p<0.001.***is p<0.001

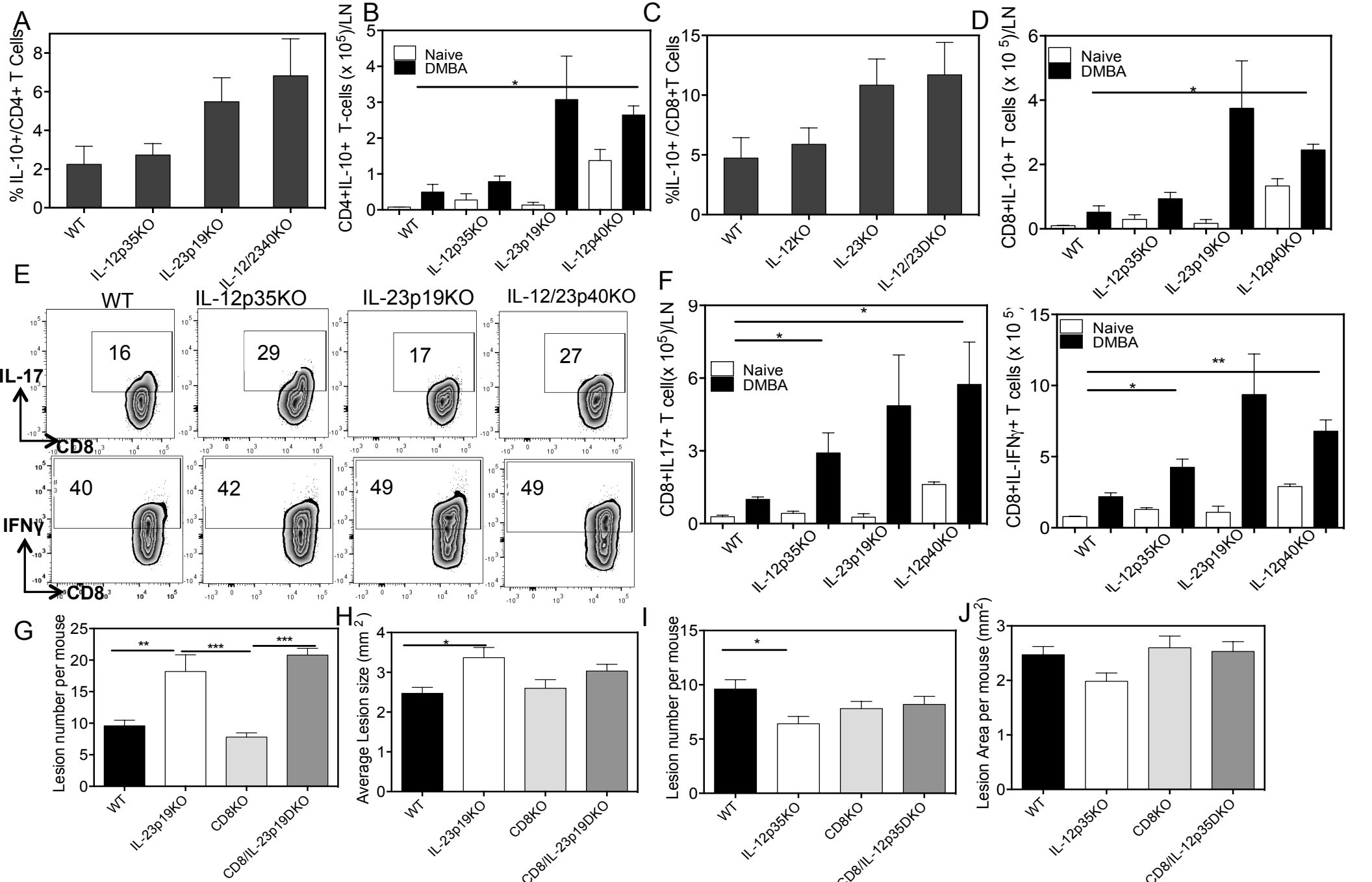

Supplementary Figure 4. (A&B) Graphs showing increase in percent CD4+IL-10+ cells **(A)** and CD4+IL-10+ T cell numbers **(B)** in IL-23p19KO and IL-12/23p40KO mice. **(C & D)** Graphs showing increase in percent CD8+IL-10+ cells **(C)** and CD8+IL-10+ T cell numbers **(D)** in IL-23p19KO and IL-12/23p40KO mice. **(E)** The percent CD8+ IL-17 and CD8+IFNγ cells was increased in IL-12p35KO and IL-23p19KO mice respectively, the number of IL-17+CD8+ cells **(F)** was increased in all of the KO mice compared to WT mice. There were increased CD8+IFNγ T cells in IL-23KO mice**. (G-I**)**Effect of CD8 loss in IL-23p19KO and IL-12p35KO mice.** *p is <0.05. ** is p<0.01. ***is p<0.001.